ORIGINAL ARTICLE

Satraplatin (JM-216) mediates G2/M cell cycle arrest and potentiates apoptosis via multiple death pathways in colorectal cancer cells thus overcoming platinum chemo-resistance

Murugan Kalimutho · Antonella Minutolo · Sandro Grelli · Amanda Formosa ·
Giulia Sancesario · Alessandra Valentini · Giorgio Federici · Sergio Bernardini

Abstract

Purposes Satraplatin acts as a potent inhibitor of proliferation in castration-resistant prostate cancer, yet the basic and molecular pharmacological mechanisms are still unknown in all types of cancer including colorectal cancer (CRC). In an effort to explain the mechanism of tumour sensitivity to satraplatin, the cytotoxic effects in a panel of CRC cell lines was examined with regard to their p53 genotype in comparison with oxaliplatin.
Methods CRC cell lines were chosen to ascertain the mechanism of satraplatin-enhanced cytotoxicity. Cells were incubated with oxaliplatin and satraplatin for 24–72 h, followed by the assessment of cell chemosensitivity with MTS. Western blot analysis was used to detect the expressions of p53-related molecules. Flow cytometry was used to monitor cell cycle perturbation while qRT-PCR to detect mRNA and miRNAs activities.
Results Satraplatin treatment resulted an elevated increase in cell death in vitro compared to oxaliplatin preceded by an acute arrest at G2/M phase, along with cyclin B1 and p21$^{waf/cip1}$ up-regulation. It also exhibited fourfold higher cellular platinum accumulations compared to oxaliplatin. Satraplatin treatment induces p53-related genes and its direct microRNA target of miR-34a independently. Thus, it potentiates apoptosis via multiple death pathways including the caspase 8 cleavages and Fas protein expression. The data suggest that the loss of p53 can increase oxaliplatin resistance but not satraplatin resistance.
Conclusion Further molecular biology studies are needed to identify the activity of satraplatin in platinum-resistant cancer models and to determine whether this orally administered platinum analogue has synergistic effects in combination with other chemotherapy agents.

Keywords Satraplatin · CRC · Apoptosis · Platinum · p53 · Oxaliplatin · miR-34a

List of Abbreviations
CRC	Colorectal cancer
DISC	Death-inducing signalling complex
miR	MicroRNA
Satraplatin	JM-216
IC	Inhibitory concentration
CRPC	Castration-resistant prostate cancer
UTR	Untranslated region
Pt	Platinum

M. Kalimutho (✉) · A. Formosa · G. Sancesario ·
A. Valentini · G. Federici · S. Bernardini (✉)
Department of Internal Medicine, University of Rome
"Tor Vergata", Via Montpellier 1, 00133 Rome, Italy
e-mail: mceric_rugan@hotmail.com

S. Bernardini
e-mail: bernardini@med.uniroma2.it

A. Minutolo · S. Grelli
Department of Experimental Medicine and Biochemical
Sciences, University of Rome "Tor Vergata", Rome, Italy

A. Minutolo · S. Grelli
Department of Laboratory Medicine, "U.O.C. Clinical
Microbiology", University Hospital Tor Vergata, Rome, Italy

Introduction

The median progression-free survival of advanced colorectal cancer (CRC) patients has increased since the introduction of oxaliplatin in combination with 5-fluorouracil–leucovorin

in systemic chemotherapy treatment. However, as a single agent, oxaliplatin has been less effective against transforming cancerous cells. Despite its proven activity in combination treatments, the acquisition of drug resistance remains a major obstacle in CRC management, ultimately leading to the death of patients [1].

Thus, many attempts have been made to scrutinize the mechanisms of chemo-resistance. The mechanisms include increased DNA repair, impaired DNA adducts formation, over-expression of copper transporters, enhanced drug detoxification and increased tolerance for DNA damage [2–5].

The p53 gene takes part in cellular responses to DNA damage by regulating cell cycle progression, cell death and DNA repair [6]. It is mutated in more than 50% of colorectal tumours [7]. Furthermore, the functional prominence of this genome guardian was correlated to cellular sensitivity and/or resistance to platinum agents. Although a clear interpretation is lacking, it has been suggested that the decreased sensitivity to platinum agents is a consequence of reduced or unfound expression of the p53 protein in these tumour models [8].

One major process leading to chemotherapy resistance is the ability of cancerous cells to evade apoptosis [9]. The development of drugs resistant cells resembles the stages of tumour progression where molecular changes cause the evolution of cancerous cells that proliferate due to their ability to escape programmed cell death [10, 11].

Thus, attempts have been made to synthesize a platinum agent with more efficient binding sites in combination with other molecules to overcome the problems that arise with current chemotherapy regimens, including oxaliplatin cross-resistance. For instance, satraplatin has been studied in a phase III clinical trial for Castration-Resistant Prostate Cancer (CRPC) [12].

Satraplatin (also known as JM-216) or bis (acetato) ammine dichloro (cyclohexylamine) platinum (IV) is the first platinum analogue available for oral administration. Satraplatin exhibits a higher cytotoxic activity in vitro when compared to other platinum compounds and also exhibits activity against some cisplatin-resistant human tumour models [13, 14].

As earlier developed platinum agents typically demonstrate significant de novo resistance and/or acquired resistance in tumour cells, satraplatin's uniqueness dwells on its putative lack of cross-resistance [15–17]. Based on preliminary cell culture investigations on various tumour types, satraplatin exhibited the ability to create DNA adducts that are more resistant to recognition by DNA nucleotide excision repair enzymes and DNA mismatch repair proteins [18–20]. Moreover, satraplatin-induced adducts are more stable and do not bind to high mobility group 1 proteins, which recognize DNA damage.

Satraplatin also inhibits trans-lesion replication by certain DNA polymerases [21]. These differences may provide a mechanism to overcome resistance to treatment observed in other platinum compounds.

In an effort to investigate the underlying mechanism associated with the cytotoxicity of satraplatin, we examined the efficacy of satraplatin compared to oxaliplatin using colorectal cancer cell lines with regard to their p53 phenotype. Moreover, to further demonstrate the mechanisms of satraplatin and its effect to overcome the chemoresistance of oxaliplatin in the absence of p53 gene, we further our analysis on three representative CRC cells exclusively one with p53 wild type (HCT116), one for mutant p53 (HT29) and the final one for p53 knockout (HCT116). We further analysed the cycle perturbation and basic molecular mechanisms of apoptosis induced by satraplatin in these cells.

Materials and methods

Drugs, chemicals and reagents

Oxaliplatin was purchased from Sigma (09512-5MG) and satraplatin was kindly gifted by Agennix AG (formerly GPC Biotech AG), Fraunhoferstr, Germany. Stock solutions of satraplatin and oxaliplatin were prepared in 0.09% saline solution stored at −20°C. Antibodies were purchased from appropriate companies as indicated: anti-p53 and anti-Bid (BD Pharmingen), anti-β-actin (Sigma), anti-Bax (Millipore), anti-BCL2 (Sigma), anti-p21$^{Cip1/WAF1}$, anti-c-ABL, anti-Fas and anti-cyclin-B1 (Santa Cruz) and anti-caspase 8 (Alexis Biochemical). Secondary antibody of anti-rabbit and mouse were purchased from Dako Cytomation, Denmark A/S. ECL detection reagents from Perkin–Elmer. miRNA analysis primer sets from Applied Biosystems.

Cell culture

HT29 were kindly provided by Dr. Isabella Faroni, University of Rome 'Tor Vergata' and HCT116, HCT116 p53$^{-/-}$ and HCT15 cells were obtained from Dr. Soddu, Regina Elena Cancer Institute, Italy. WiDr and LoVo cells were given by Dr. Rossana Supino from Instituto Nazionale Tumori, Milan, Italy and HCT116 p21$^{-/-}$ were obtained from Prof. Bert Vogelstein, from Ludwig Centre at John Hopkins, USA. All the cell lines were tested for mycoplasma infection and were grown in monolayer cultures in DMEM (HCT116, HCT116 p53$^{-/-}$, HT29, HCT116 p21$^{-/-}$), DMEM: F12 (WiDr), RPMI 1640 (HCT15) and Ham's Nutrients mix F12 (LoVo) supplemented with 10–20% FBS and 1% penicillin streptomycin according to

UKCCCR guidelines [22]. No antibiotics were added to the medium prior to the treatment. The cells were trypsinized and passed once a week and all the experiments were conducted at early passages.

Cytotoxicity evaluation assay

The concentration of oxaliplatin and satraplatin resulting in 50% inhibition of control growth (IC_{50}) was calculated with an MTS assay (Promega). Three thousand cells per well were seeded in 96-well plates and 24 h later the cells were exposed to 200 μl of 0–250 μM oxaliplatin and satraplatin. After 72 h of incubation, 20 μl of MTS solution was added and the IC_{50} concentrations were calculated using CalcuSyn version 2.0. Since this analysis is concerned with a comparison between oxaliplatin and satraplatin, the analysis was done with drug concentrations controlled to be below IC_{50} value (10 μM) for practical considerations. At this concentration for both drugs, the percentage cell death lies between 20 and 40% for all cell lines tested.

Intracellular platinum quantification

Intracellular platinum (Pt) levels were measured following 2 h incubation with 6.25, 12.5, 25, 50 and 100 μM of satraplatin or oxaliplatin. Approximately 1×10^6 cells were washed twice with 5 ml of cold phosphate-buffered saline (PBS) and the monolayer was scraped into 2 ml PBS. Cellular Pt content was determined by flameless atomic absorption spectroscopy (FAAS) using a Perkin–Elmer AAnalyst 800 (Beaconsfield, Bucks, UK). Cell aliquots were dissolved in 0.2% nitric acid and automatically injected into the graphite furnace. The concentration of Pt in ng/ml was measured by comparing Pt standards ranging from 5 to 500 ng/ml. Under these conditions, the limit of detection was between 5 and 10 ng Pt/ml. The cellular platinum contents were then expressed as nmol Pt/ml normalized to 1×10^6 cells.

Cell cycle analysis

For cell cycle analysis 5×10^4 cells of HCT116, HCT116 p53 null and HT29 were seeded in six-well plates in triplicate and allowed to attach for 24 h. For time response studies, cells were treated with 10 μM satraplatin and oxaliplatin for 48 h and 72 h. Both attached and floating cells were harvested, washed twice with 1 ml of PBS and re-suspended in PBS containing 10 mg/ml of RNAse and incubated for 1 h. Later, 10 mg/ml propidium iodide (Sigma p4170-100 mg) was added prior to the analysis. Cells were analysed for DNA content using a FACScan flow cytometry (BD Biosciences, Mountain View, CA).

The proportion of cells in G0/G1, S phase and G2/M were quantified using CellQuest^{TM} software (BD Biosciences, San Jose, CA). The software directly calculated the percentage of cells in each phase.

Evaluation of apoptosis

For apoptosis assays, cells were plated in six-well plates and treated with 10 μM of satraplatin or oxaliplatin. Isolated nuclei were then analysed after 24, 48 and 72 h of treatment, using a FACScan flow cytometry (BD Biosciences, Mountain View, CA) as previously described [23]. Briefly, detectors and amplifier gains for forward and orthogonal scatter were adequately selected in order to simultaneously detect nuclei from viable, apoptotic and necrotic cells. Events were gated on forward versus orthogonal scatter in such a way that degraded DNA from cell debris or from doublets was excluded and nuclei from viable, apoptotic and necrotic cells were assayed. Data acquisition and analysis was performed using CellQuest^{TM} software (BD Biosciences, San Jose, CA) on a minimum of 5,000 events for each samples. The second method for evaluation of apoptosis consisted in double staining of the cells with fluorescent annexin-V and with PI solution for the FACS data confirmation. To this purpose, the "Annexin-V-FITC Apoptosis Detection Kit" (BD-Bioscience Pharmingen, San Diego, CA, USA) was used according to manufacturer instructions. Briefly, 5×10^5 cells were incubated for 15 min with annexin-V-fluorescein isothiocyanate (FITC) and then washed in annexin buffer. Cells were then stained with PI solution and analysed immediately after staining by flow cytometry using a FACScan flow cytometry and Cell Quest^{TM} software. This method is widely accepted to distinguish between early apoptosis and necrosis.

Quantitative PCR

RNA isolation, cDNA synthesis and RT-PCR

Total RNA was isolated with TRIzol reagent (Invitrogen, CA). The integrity of total RNA was determined by 1% agarose gel electrophoresis. cDNA synthesis was carried out with the Superscript III cDNA synthesis kit (Invitrogen, CA) using 1 μg of total RNA as the template and specific reverse primers (Table 1) according to manufacturer instructions. The PCR amplification was carried out in a final volume of 25 μl containing 12.5 μl of SYBR green (2×), 0.5 μl both primers (10 μM), 1 μl of cDNA. Cycling conditions included preheating at 95°C for 10 min and then 40 cycles of: 95°C for 30 s, 60°C for 30 s and 72°C for 45 min, followed by standard dissociation curve. Analysis below 35 cycles was considered for the $2^{-\Delta\Delta Cq}$ calculation according to the MIQE guidelines [24].

Table 1 Primers list for mRNA RT-PCR

Genes	Primer set	Length (bp)
MLH1	Forward: 5′ TTTACAACATAGCCACGAGGA 3′	221
	Reverse: 5′ CTATCAGTTCTCGACTAACAGCA 3′	
P21$^{waf1/cip1}$	Forward: TCACACCATGACAAGACTCTC	281
	Reverse: AAATGCCAGTCACTTAGTACAG	
PMS2	Forward: 5′ CTCATAGCACCTCAGACTCTC 3′	140
	Reverse: 5′ GGAAATCAGTTTAGCCCTTTCAG 3′	
BCL2	Forward: 5′ GGATTGTGGCCTTCTTTGAG 3′	205
	Reverse: 5′ CCAGGAGAAATCAAACAGAGG 3′	
BRCA1	Forward: 5′ CTGCTCAGTAATGAACACTGG 3′	218
	Reverse: 5′ CAGCATCCATTGAGAATCCC 3′	
B2M	Forward: 5′ CAGCGTACTCCAAAGATTCAG 3′	110
	Reverse: 5′ GTCAACTTCAATGTCGGATGG 3′	
MSH2	Forward: 5′ TTCCATACAGAGGAAACTAGGAC 3′	300
	Reverse: 5′ AACTGCAACCTGATTCTCCA 3′	
BAX	Forward: 5′ TTTGCTTCAGGGTTTCATCC 3′	145
	Reverse: 5′ TGTTACTGTCCAGTTCGTCC 3′	
Tp73	Forward: 5′ AAACCCAGACTTATCTCAGACAG 3′	130
	Reverse: 5′ GTCTTGCTGCCATATACACC 3′	
ERCC1	Forward: 5′ AATTTGGCGACGTAATTCCC 3′	169
	Reverse: 5′ GGGATCTTTCACATCCACCT 3′	
14-3-3-sigma	Forward: 5′ CTCAGTAGCCTATAAGAACGTG 3′	250
	Reverse: 5′ AGTAGTCACCCTTCATCTTCAG 3′	
CLU	Forward: 5′TGATCCCATCACTGTGACGG	120
	Reverse: 5′ GCTTTTTGCGGTATTCCTGC	
β-actin	Forward: 5′ GGACTTCGAGCAAGAGATGG 3′	242
	Reverse: 5′ AGCACTGTGTTGGCGTACAG 3′	
Tp53	Forward: 5 GTCTGGGCTTCTTGCATTCT 3′	120
	Reverse: 5′ AATCAACCCACAGCTGCAC 3′	
GADD45	Forward: 5′ GAGAACGACATCAACATCCTG 3′	152
	Reverse: 5′ GAATGTGGATTCGTCACCAG 3′	

miRNA reverse transcription and qRT-PCR analysis

Enriched microRNAs were extracted with mirVana™ Isolation Kit (Ambion Inc., TX). Based on TARGET scan and PIC target, miRNAs that target our molecules were selected. Based on the top predicted target, we identified 14 miRNAs involved with our selected gene group focusing on cell cycle analysis, cell death and DNA repair system. Applied Biosystems qRT-PCR primer sets for miRNA specific reverse transcription including hsa-miR-150 (→p53/ERCC1), hsa-miR-152 (→MLH1/GADD45), hsa-miR-128a (→MLH1/BAX), hsa-miR-34a (→BCL2), hsa-214 (→BAX), hsa-miR-218 (→BRCA1), hsa-miR-21 (→MSH2), hsa-miR-106a (→p21), hsa-miR-20, hsa-miR-148a (→GADD45), hsa-miR-370 (→CLU), hsa-miR-326 (→Tp73), hsa-miR-128b, hsa-miR-17-3p and endogenous control RNU19 and RNU6B were utilized according to the manufacturer's protocol. Briefly, the reaction master mix containing 5× RT buffer, 5× RT primer, Array-Script™

Enzyme Mix and nuclease-free water was mixed with 50 ng of input microRNA. The mixture was incubated for 30 min at 37°C, and then 10 min at 95°C. qPCR was carried out using the Stratagene Real-Time PCR System and Applied Biosystems qRTPCR miRNA Detection Kit (Ambion Inc. TX). The PCR master mix contains Applied Biosystems 2× PCR buffer (with FAM-labelled Taqman probe), 1 μl FAM-labelled specific primers and cDNA from process miRNA. RT products was processed as follows: 95°C for 10 min and then 95°C for 15 s and 60°C for 30 s for up to 40 cycles ($n = 2$). Gene expression was calculated via a $2^{-\Delta\Delta Cq}$ method.

Western blotting

All cells were seeded in 75 cm² flasks and treated with 10 μM oxaliplatin or satraplatin for 24, 48 or 72 h, then rinsed with PBS twice, harvested and re-suspended in 150 ml of Chaps 0.1% lysis buffer (1 M Tris–Cl pH 7.5, 5 M NaCl, 10%

CHAPS, ddH$_2$O). The cells suspension was vortexed and kept on ice for 30 min before cell debris was pelleted and the supernatant transferred to a new tube. SDS–polyacrylamide gel electrophoresis sample loading buffer was added to 20 µg aliquots, heated at 95°C for 5 min and then loaded on 10% Tris–HCl gels (BioRad, Hercules, CA, USA). Proteins were transferred to a nitrocellulose membrane (Amersham, Piscataway, NJ, USA) and blocked with 1% non-fat milk and 1% BSA for at least 2 h. Membranes were then probed at 4°C with the appropriate primary antibody in 0.1% T-TBS overnight with the following antibodies: anti-p53 (1/500), anti-p21$^{Cip1/WAF1}$ (1/200) and anti-β-actin (1/1000), anti-Bax (1/500), anti-BCL2 (1/200), anti-c-ABL (1/200), anti-Fas (1/500), anti-cyclin-B1 (1/200), anti-caspase 8 (1/500) and anti-Bid (1/500). Membranes were washed three times with washing buffer (PBS with 0.1% Tween-20 for 10-min interval). Then, the filter was probed with the appropriate peroxidase-conjugate secondary antibody for 1 h (from DakoCytomation, Denmark A/S). The secondary antibody was washed three times with washing buffer and the signal was developed using ECL Plus Western Blotting Detection Method (Perkin–Elmer). Detection was carried out using a Molecular Imager ChemiDoc XRS System, Bio-Rad laboratories (UK) Ltd. Protein levels were standardized using the signal from the β-actin probe.

Statistical analysis

The gene expression ΔCq values of mRNA and miRNAs from each sample were calculated by normalizing with internal control of ACTB and B$_2$M (for mRNA) and RNU19 and RNU6B (for microRNAs) and relative quantitation values were calculated according to the $2^\wedge - \Delta\Delta$Cq method. The statistical studies were performed using a statistical software system (SPSS, version 12.0 for windows, Chicago, IL, USA). The statistically significant differences in expression level between control and treated samples for each target were calculated using a paired Wilcoxon test. Comparison of mean values of proliferation and apoptosis levels in response to satraplatin and oxaliplatin treatment was carried out using the Bonferroni post hoc multiple comparisons ANOVA test. $*p \leq 0.05$ value was considered significant while $**p \leq 0.001$ value was considered highly significant.

Results

Cytotoxic effect of satraplatin in the panel of colorectal cancer cells

In order to evaluate the effective drug concentrations, a panel of six CRC cell lines with different p53 genotypes were treated with various concentrations (ranging from 0 to 250 µM) of oxaliplatin or satraplatin for 72 h, before MTS assay. The IC$_{50}$ value of each cell line is shown in Table 2. The IC$_{50}$ value ranged from 13 to 27 µM for satraplatin, and from 19 to 96 µM for oxaliplatin. All p values between these two treatment groups showed a significant difference in IC$_{50}$ value except in HT29 cells where there was no significant difference as shown in Table 2. The general trend of MTS assays for HCT116, HCT116 p53$^{-/-}$ and HT29 cells are shown in Fig. 1.1 (A–C). In all three cell lines, satraplatin showed a higher percentage of cell inhibition based on MTS assay, compared to oxaliplatin. For example, there was a statistically significant difference between both drugs at doses from 10 to 50 µM in HCT116, $p = 0.001$. Figure 1.2 (a–f) shows that the cell morphological changes at 10 µM of both drugs in two of the cell lines tested as described in the figure legend.

To investigate the consequences of satraplatin treatment on cell cycle and apoptosis, we used three different CRC cell lines with different p53 status; HCT 116 (wild type), HCT 116 (p53$^{-/-}$) and HT29 (mutant).

Satraplatin treatment results in higher accumulation of platinum in CRC cells, compared to oxaliplatin

To investigate the cellular contents of Pt in our model, we assessed different concentrations of drug (0–100 µM) based on FAAS. Following the exposure of satraplatin and oxaliplatin, the accumulation of satraplatin was higher in the cells tested compared to oxaliplatin (Fig. 2). For instance, when the cells were treated with 100 µM of both drugs accumulation of satraplatin was 387.4 ng/ml versus 29.13 ng/ml for oxaliplatin in HCT116 cells, 316 ng/ml for satraplatin versus 18.96 ng/ml for oxaliplatin in HCT16 p53$^{-/-}$ cells. Based on this graph, we found that the platinum incorporation into cells at 10 µM, which was the evaluation dosage for the subsequent experiments, was

Table 2 IC$_{50}$ value of satraplatin and oxaliplatin in a panel of colorectal cancer cell lines

Cell line	Tp53 status	IC$_{50}$ µM		IC$_{50}$ p values*
		Satraplatin	Oxaliplatin	
HCT116	Wild type	15.7 ± 0.5	21.5 ± 1.3	0.0020
HT-29	Mutant	27.2 ± 3.1	33.1 ± 2.7	0.1199
HCT116 p53$^{-/-}$	Knockout	14.4 ± 1.6	95.7 ± 2.7	0.0001
WiDr	Mutant	26.9 ± 2.4	36.2 ± 2.3	0.0084
LoVo	Wild type	16.3 ± 1.3	19.4 ± 0.9	0.0274
HCT15	Mutant	13.3 ± 1.1	20.4 ± 2.3	0.0085

* p value represents difference in IC$_{50}$ between satraplatin and oxaliplatin treatment

Fig. 1 Effect of satraplatin and oxaliplatin on cytotoxicity of representative colorectal cancer cells. MTS assay curve demonstrating cytotoxic effect on both drug treatment. 1.1 *a–c* Curves representing the average value for at least three independent experiments in quadruplicate. Cells were treated for 72 h with increased concentration of both drugs as described in 'Materials and methods'. 1.2 Cell morphology after 10 μM exposure of satraplatin and oxaliplatin in HCT116 and p53 null. Representative results are shown for HCT116 untreated ctrl (1.2*a*) HCT116 oxaliplatin (1.2*b*) and HCT116 satraplatin (1.2*c*), p53 null untreated ctrl (1.2*d*), p53 null oxaliplatin (1.2*e*) and p53 null satraplatin (1.2*f*) cells at 72 h after treatment. *Arrows* shows typical morphology of cell undergoing apoptotic. Cells were treated as detailed in 'Materials and methods'
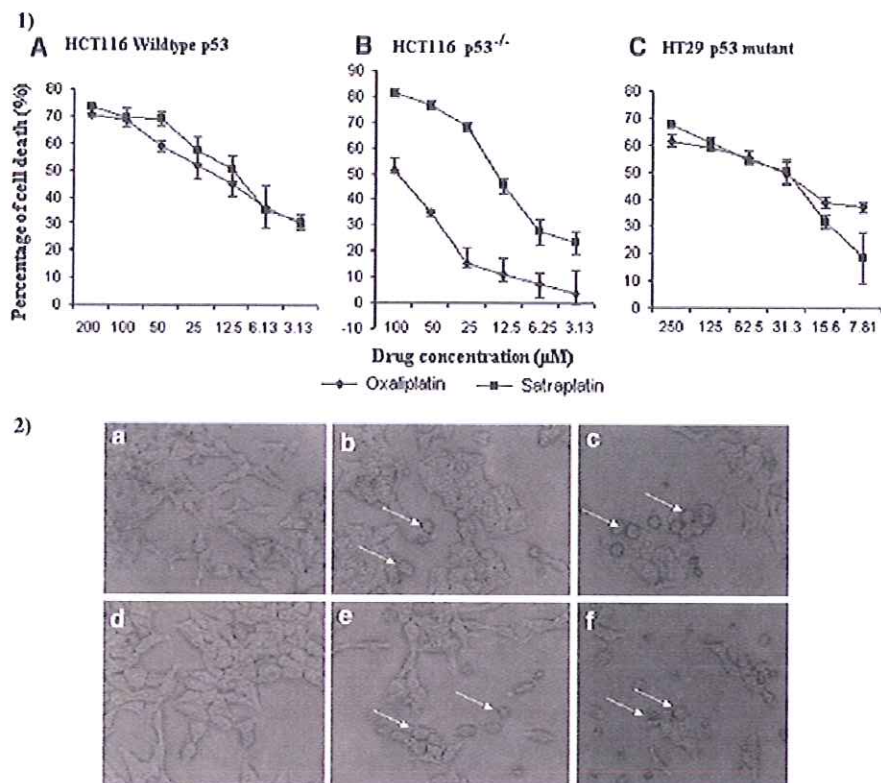
approximately fourfold higher for satraplatin compared to oxaliplatin.

Treatment of CRC cells with satraplatin and oxaliplatin alters cell cycle profile

To analyse the effect of satraplatin and oxaliplatin treatment on cell cycle, we treated CRC cells with 10 μM of each drug for 48 or 72 h. The cell cycle analysis of three CRC cell lines following treatment with oxaliplatin and satraplatin are shown in Table 3.

Satraplatin noticeably increased the relative number of cells in G2/M phase (57.08% vs. 14.42% for untreated cells at 72 h, **$p < 0.001$) in HCT116 cells while a minor alteration was observed with oxaliplatin treatment. We also observed a similar alteration of cell cycle in p53$^{-/-}$ HCT116 cells following satraplatin treatment (50.85% vs. 28.52% for untreated control at 72 h, **$p < 0.001$), while a similar pattern of cell perturbation was observed with oxaliplatin treatment at 72 h where the cells accumulated in S phase. On the other hand, in HT29 cells both drug treatments induced S phase cell cycle arrest, Table 3.

Satraplatin induces apoptosis in CRC cells

To assess the effect of satraplatin treatment on apoptosis, the three CRC cell lines were treated with 10 μM satraplatin

and oxaliplatin for 24, 48 and 72 h and apoptosis was assessed by flow cytometry. The results shown are the mean values ± standard error (SE) obtained from three independent experiments.

In HCT116 cells, no significant increase in apoptosis was detected following treatment with satraplatin for 24 h, compared to untreated and oxaliplatin treated cells (data not shown). However, following treatment for 48 h and 72 h, a substantial increase in sub-G1 population was detected when compared to untreated cells (48 h: 2.8-fold changed vs. to untreated control; 72 h: 10.9-fold changed with satraplatin vs. 7.7-fold changed with oxaliplatin to untreated control, $p < 0.001$ (Fig. 3). A similar apoptotic profile was also observed in HT29 and HCT116 p53$^{-/-}$ cells, although the difference between satraplatin and oxaliplatin was also profound in HT29 cells following 48-h and 72-h treatment. There were significant differences of apoptosis profile between these three cell lines tested as shown in Fig. 3.

We confirmed these results by counting annexin-V-PI cells following satraplatin treatment. This method also allowed us to detect early apoptotic (annexin-V+/PI−) and late apoptotic/necrotic (annexin-V+/PI+) cells [23].

In HTC116 cells, 24 h of treatment with 10 μM satraplatin, resulted in 0.20% annexin-V+PI+ cells and 22.67% annexin-V+/PI− cells versus 0.14% annexin-V+PI+ cells and 7.55% annexin-V+/PI− cells with
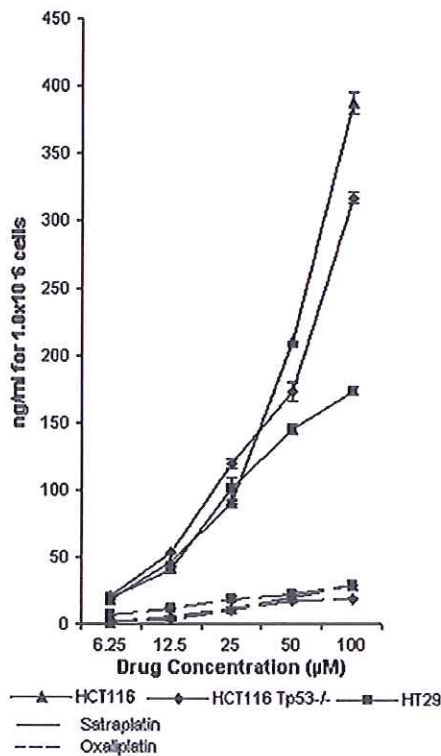
Fig. 2 Quantification of cellular platinum accumulation by Atomic Absorbance Spectrophotometer (AAS) following 2-h incubation of satraplatin and oxaliplatin (drug concentration range: 6.25–100 μM). *Direct line* indicates satraplatin and *dot line* indicates oxaliplatin treatments. Satraplatin in comparison with oxaliplatin resulted in more accumulation of Pt in each cell line tested in reference to p53 gene status. This demonstrates that the uptake of platinum is more efficient with satraplatin than oxaliplatin. Based on 10 μM treatment with both drugs, the accumulation of satraplatin was 35–40 ng/ml whereas with oxaliplatin only expected 3–10 ng/ml platinum for 10^6 cells. The accumulation of satraplatin in the cells was fourfold higher than after oxaliplatin treatment. *Error bars* SE of two independent experiments

oxaliplatin treatment, while in untreated controls 0.23% annexin-V+PI+ and 9.32% annexin-V+/PI− cells were observed. Similar results were obtained in HT29 mutant cells and in $p53^{-/-}$ cells as showed in Fig. 4, which demonstrates the efficacy of satraplatin on cell death induction when compared to oxaliplatin.

These data also indicate that satraplatin induces cell death in cells mainly, if not exclusively, by apoptosis, with no or very little contribution by necrosis.

To study the biological effect of satraplatin on CRC cells cytotoxicity, cell cycle distribution and apoptosis, first we analysed the p53 protein expression since our models differ in p53 status. We observed a significant increase in p53 protein expression after 48 h of treatment of both drugs in HCT116 cells whereas no p53 protein accumulation was observed in HT29 cell line as shown in Fig. 5a.

We observed a down-regulation of p53 protein expression with both treatments in HT29 cell line. No p53 expression has been shown in HCT116 $p53^{-/-}$ cell line as expected. To clarify p53 expression and the action of its downstream genes dependent and independently based on these drugs treatment, first we analysed gene expression patterns at mRNA levels.

Satraplatin initiates p53 signalling pathway independently

To further investigate the molecular cascade of events following the exposure to both drugs, we selected appropriate genes involved in cell cycle regulation, DNA damage response and transcription factor control based on the p53 signalling pathway. Using this small array with a 15-gene simultaneous analysis after 48 h of treatment, we detected significant changes in mRNA modulation. We detected a minor alteration in p53 mRNA levels in HCT1116 (satraplatin: 1.6-fold, $p = 0.016$ vs. oxaliplatin: 1.53-fold, $p = 0.007$) but not in HT 29 (satraplatin: −1.05-fold vs. oxaliplatin: −1.07-fold). We also detected the changes in expression levels of ERCC1, MSH2, BRCA1, GADD45, CLU and Bax genes (Table 4). BCL2 expression was much more down regulated in HCT116 cells with twofold lower than oxaliplatin treatment whereas 12-fold lower in $p53^{-/-}$ cells. Table 4 shows the fold-changed expression level in the three cells tested. Furthermore, we noticed an up-regulation in Bax gene expression, further suggesting the apoptosis induction in these cells by p53-dependent and independent manner.

Effect on the levels of cell cycle-related protein expression

To elucidate the role of cell cycle regulating proteins, we investigated the expression of cyclin B1 involved in G2/M cell cycle arrest. We found a marked increase in cyclin B1 in HCT116 and p53 null cells exposed to 48-h satraplatin. A very low expression was detected by oxaliplatin in HCT116 wild type and null p53 lines, whereas we could detect the same expression for HT29 by both drugs (Fig. 5b). We also detected a marked increase in p21 expression at 48 h in HCT116 and the expression is much higher with satraplatin treatment than oxaliplatin (Fig. 5c). To confirm the G0/G1 arrest by oxaliplatin, we looked at the expression of c-ABL gene. The expression is much higher after oxaliplatin than after satraplatin treatment in HCT116 and null p53. This might suggest that the G0/G1 block was activated upon the treatment with oxaliplatin, whereas very low expression was detected after satraplatin treatment (Fig. 5c).

Table 3 Effect of satraplatin and oxaliplatin on cell cycle perturbation in representative colorectal cancer cells at 10 μM

	HCT116			HCT116 Tp53$^{-/-}$			HT29		
	Untreated	Oxaliplatin	Satraplatin	Untreated	Oxaliplatin	Satraplatin	Untreated	Oxaliplatin	Satraplatin
48 h									
G0/G1	69.95	56.04	23.13**	67.47	65.32	26.56**	62.2	37.52*	17.64**
S	17.56	25.94	26.28	11.33	21.29	52.32**	34.94	53.58	51.89*
G2/M	13.49	18.02	50.59**	21.37	13.29	21.08	2.86	8.9	30.47**
72 h									
G0/G1	69.55	57.48	21.05**	58.86	40.54	13.58**	42.93	11.13*	10.01**
S	17.03	19.15	21.88	12.9	52.56**	35.95*	53.68	84.64**	68.87*
G2/M	14.42	24.37	57.08**	28.52	7.03	50.85**	2.39	4.23	31.12

Results are representative of at least three independent experiments. This data demonstrated that satraplatin treatment arrested cell in G2/M phase in wild type p53, and full S phase arrest in mutant p53 cells

Treatment versus untreated CTRL

* $p < 0.05$

** $p < 0.001$
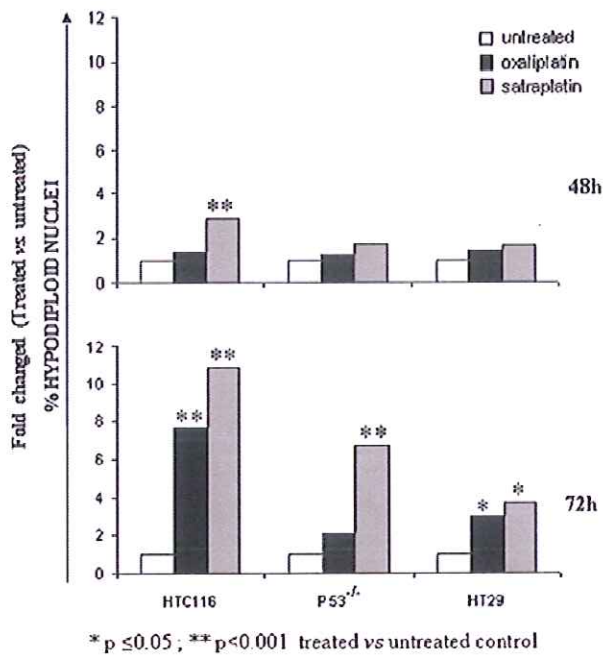
Fig. 3 Apoptosis analysis using PI as described early by us [23] on representative colorectal cell lines after the treatment with 10 μM of satraplatin and oxaliplatin for 48 h and 72 h. The results are the means ± SE of the percentage of hypodiploid nuclei analysed by flow cytometry PI detection. In all three cell lines, an increase in apoptosis cells were detected based after satraplatin compared to oxaliplatin treatment

Effect on the levels of cell death pathway related protein expression

Bax relocation to the mitochondrial, accumulation of cytochrome c in the cytoplasm, caspase 8 activation and Bcl2 down-regulation are all events consisted with intrinsic pathway of apoptosis activation. To elucidate the mitochondrial associated apoptosis molecules, Bcl2 and Bax protein expression was noticed in our cell models. Bcl2 expression in both HCT116 and p53 null cells was much more reduced after 48 h with satraplatin than oxaliplatin treatment. No Bcl2 protein expression was detected in HT29 with the same result as gene expression. On the other hand, the expression of Bcl2 on oxaliplatin treatment was significantly reduced but a greater reduction was observed with satraplatin treatment (Fig. 6a, d). This further suggests that satraplatin-induced apoptosis might be by p53-dependent as well as by p53-independent manner. We also detected Bax protein expression as well as an activation of truncated Bid in all the cells tested. Fas protein expression was detected by both drug treatments mainly in HCT116 cells suggesting that these cells might also undergo Fas-induced apoptosis (Fig. 6a). To further illustrate the activation of caspase family, we choose pro-caspase 8 in our analysis. Pro-caspase 8 cleavage was observed with satraplatin treatment whereas only a very low signal with oxaliplatin treatment (Fig. 6b).

Differential expression of miR-34a exhibits apoptosis signals in CRC cells

We conducted a differential miRNA expression analysis after satraplatin- and oxaliplatin-based treatments. The expression of miR-34a which target molecule is Bcl2 is higher after satraplatin than oxaliplatin treatment in HCT116 cells (2.65- vs. 1.89-fold). While a down-regulation of miR-34a levels was observed in HT29 cells for both drug treatments, in p53 null cells, we observed a 1.69-fold up-regulation with satraplatin, while a down-regulation was observed with oxaliplatin treatment (Fig. 6c). For both
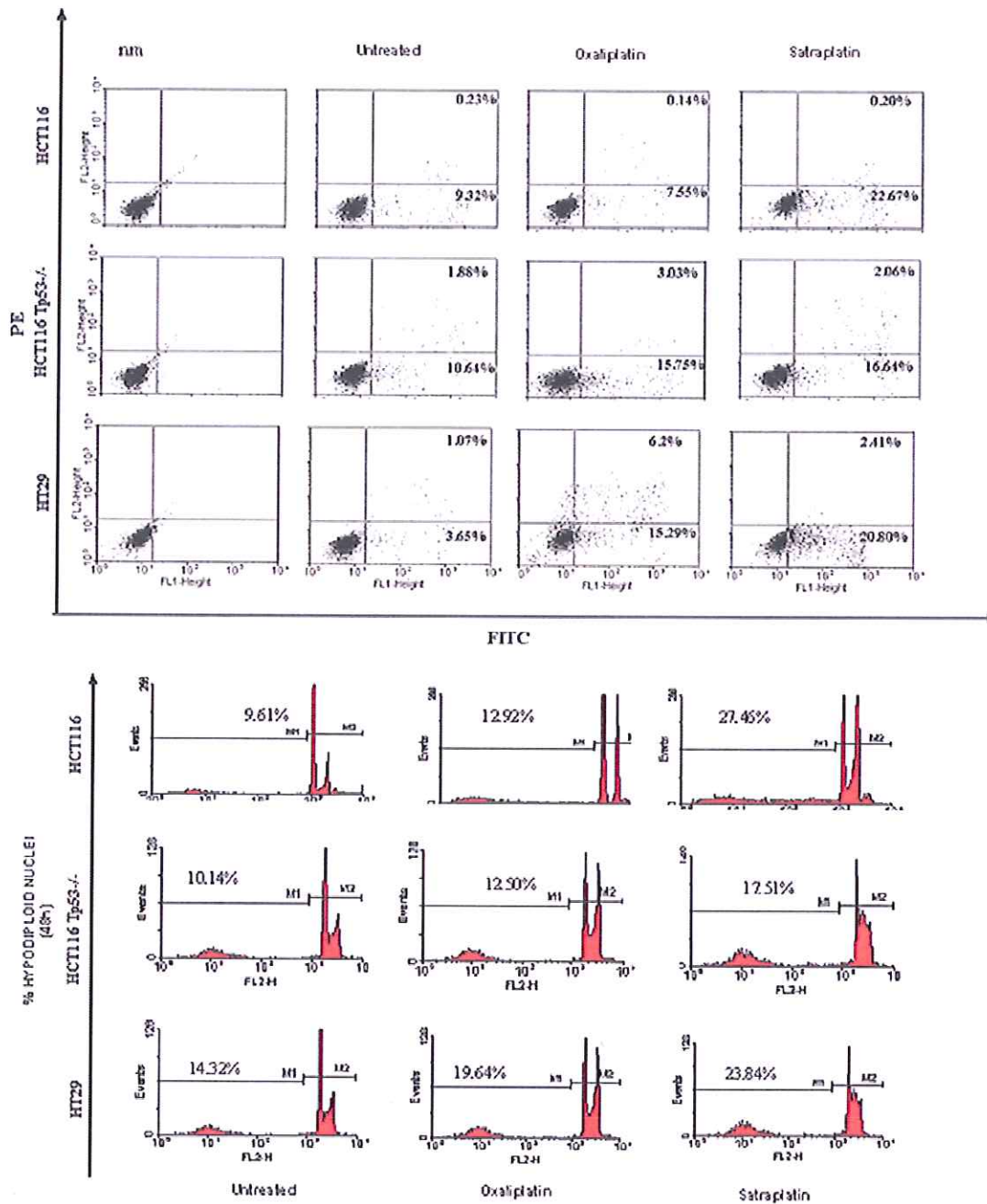
Fig. 4 Evaluation of apoptosis analysis in representative colorectal cell lines after the treatment with 10 μM of satraplatin and oxaliplatin for 24 and 48 h by annexin-V/PI assay. The results are the means ± SE of the percentage of hypodiploid nuclei analysed by flow cytometry after 24 h of annexin in relation to 48 h of PI detection. Comparable analysis was done to detect the apoptosis percentage based on both drugs treatment from two independent experiments. Typical cytograms demonstrating satraplatin induces high levels of apoptotic cells compared to oxaliplatin treatment at the same drug concentration

drugs, we also detected a down-regulation of hsa-miR-214 that targets the UTR of Bax gene. HCT116 and HT29 cells also exhibited a down-regulation of hsa-miR-214 but very low expression was observed in HCT116 p53 null cells. The differential expression of other miRNAs analysed was pronounced in Table 4.

Discussion

Colorectal cancer demonstrates elevated resistance to chemotherapy agents compared with other human malignancies [25]. However, in a combination of 5-fluorouracil–leucovorin–oxaliplatin patients have gradually achieved
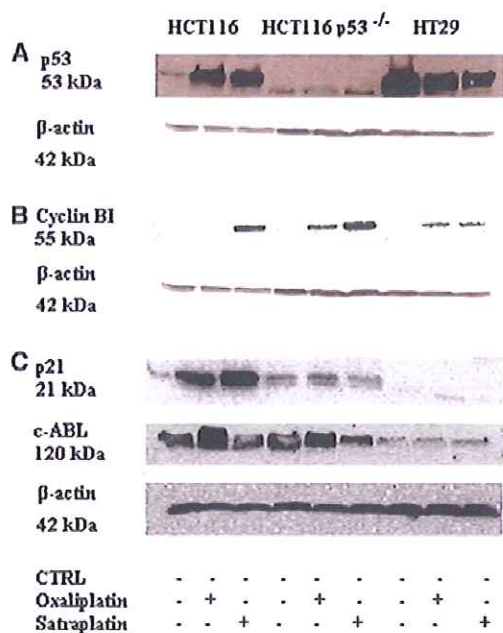
Fig. 5 Effect of oxaliplatin and satraplatin on p53 protein and cell cycle-related protein levels in a panel of wild type, knockout and mutant p53 gene carrying cells. Blot for actin served as loading control. a Over-expressed p53 protein by satraplatin and oxaliplatin treatment in HCT116 while reduced expression levels were observed in HT29 cells with both treatments. b Expression of p53 downstream genes, p21$^{waf/cip1}$, and cyclin B1, c-ABL were examined following 48 h of treatment with both drugs at 10 μM concentration. The expression of p21$^{waf/cip1}$ is higher with satraplatin treatment while c-ABL expression was higher with oxaliplatin treatment. c The expression of cyclin B1 is evidenced at 48 h when the expression is stronger with satraplatin treatment in HCT116 and p53 null cells while same levels of expression were observed with oxaliplatin treatment in HT29 cells

improvement in clinical outcomes along with increased median progression-free survival [26]. Despite this improvement, most platinum compounds eventually suffer from de nova resistance or acquired resistance to the treatment over the time. In this study, we showed the effects of oxaliplatin versus an orally administered platinum drug, satraplatin in CRC cell lines which differ in p53 status on fundamental cellular pharmacological levels.

As documented before for prostate and other cancers [27, 28], satraplatin exhibited comparable anti-proliferation effects on cell growth. Demonstrations of anti-proliferation effect on our clonogenic model further support the action of satraplatin in a p53-dependent and p53-independent manner.

There was a significant discrepancy in the uptake of platinum into the cells across the three cell lines investigated. When we examined the contents of 10 μM of both drugs, the intracellular Pt levels were fourfold higher with satraplatin. The cells displayed a greater ability to tolerate higher levels of Pt with satraplatin compared to oxaliplatin.

This may be due to the greater lipophilicity of satraplatin enhancing its intracellular accumulation.

Flow cytometry analysis revealed that a slowdown in S phase transit was a prominent cell cycle effect of satraplatin in these cells. This was accompanied by a marked accumulation of cells in G2 phase in HCT116 and p53 null cells after 72 h. However, in HT29 cells, the majority of the cells were still in S phase with no evidence of build up of cells in G2 phase at this point. Similar cell cycle perturbations were observed with cisplatin [29] and other platinum agents [30, 31]. Taken together, these data indicate that the accumulation of cells in S phase is a general cell cycle effect of platinum drugs and depending on the nature of the cell type as well as based on dose dependent which showed to be associated with G2 cell cycle arrest [30–32]. In the p53 wild type and p53 null cells, accumulation of cells in G2 coincided with the point at which significant apoptosis was occurring at 48 and 72 h. It has been suggested that G2 arrest facilitates repair of DNA damage prior to mitosis and depending on the success of repair or extent of DNA damage, cells emerging from G2 either begin to cell cycle normally or engage in apoptosis [33, 34]. Our data suggest that the latter may be occurring in the HT29 cells, despite the repair of Pt lesions induced by satraplatin.

Relatively more apoptotic cells were measured after satraplatin than oxaliplatin treatment suggesting that satraplatin is a stronger inducer of apoptosis. To confirm our apoptosis data measured by hypodiploid nuclei assessed by PI staining, we evaluated the percentage of annexin and PI which the values were quite similar. When we correlated our apoptosis data with the p53 gene status, we observed that even if HT29 cells that have reduced p53 protein expression, satraplatin still induced apoptosis. This suggests that the differences of p53 status in the cells play a role in the cell cycle arrest and apoptosis inductions and adds further weight to the evidence that this process may be p53 dependent as well as p53 independent.

The cell cycle determination and their validation at the protein level suggested that two different mechanisms are responsible for oxaliplatin-induced G1 and satraplatin-induced G2 transition control. Satraplatin induced an elevated protein expression of cyclin B1 after 48 h compared to oxaliplatin. It is now widely accepted that the G2/M transition is partly governed by the CDK1-cyclin B complex [35, 36]. Another fact is that p21$^{waf1/cip1}$ exerts a key role in controlling the G2 arrest by inhibiting the CDK1-cyclin B complex. Protein analysis showed that p21$^{waf1/cip1}$ expression was up regulated under both drug treatments. Based on this data we assumed that the p21$^{waf1/cip1}$ pathway may be involved in early events of the satraplatin-induced G2 block and vice versa. Hata et al. [37] has also suggested that p21$^{waf1/cip1}$ might play a role in exerting the

**Table 4** mRNA and miRNA of satraplatin versus oxaliplatin at 48 h post-treatment

No.	Gene symbol	HCT116		HCT116 p53$^{-/-}$		HT29	
		Oxaliplatin	Satraplatin	Oxaliplatin	Satraplatin	Oxaliplatin	Satraplatin
Fold change (mRNA) to untreated CTRL							
1	ERCC1	2.41	1.78	1.18	1.11	1.25	1.14
2	MLH1	1.45	1.22	1.61	1.38	1.05	−1.29
3	MSH2	−3.13	−1.7	1.8	1.23	2.13	1.37
4	p53	1.53	1.6	ND	ND	−1.07	−1.05
5	BRCA1	−2.8	2.36	−1.44	−1.55	1.19	1.47
6	PMS2	2.2	1.44	−1.26	−1.05	1.38	1.31
7	Tp73	1.3	1.49	1.39	1.66	1.37	−1.12
8	GADD45	2.57	1.88	1.6	1.2	1.09	1.45
9	p21	2.39	1.83	1.31	1.99	1.04	1.09
10	BCL2	−2.68	−4.33	−1.29	−13.38	ND	ND
11	BAX	2.59	2.18	1.06	1.13	1.2	1.22
12	14-3-3-SIGMA	3.96	4.77	−2.39	1.6	−1.51	1.42
13	CLU	1.17	2.67	−1.77	2.22	1.94	3.42
Fold change (miRNA) to untreated CTRL							
1	hsa-miR-150 → Tp53/ERCC1	1.61	2.06	−2.04	−1.31	−2.56	−1.04
2	hsa-miR-152 → MLH1/GADD45	1.34	2.53	−1.53	2.05	−1.21	1.64
3	hsa-miR-128a → MLH1/BAX	1.41	−1.04	1.07	−1.06	−1.41	−3.01
4	hsa-miR-34a → BCL2	1.89	2.66	−1.24	1.69	−1.33	−1.84
5	hsa-miR-214 → BAX	−1.06	−1.48	−2.21	−2.78	−1.17	−1.18
6	hsa-miR-218 → BRCA1	−1.58	−1.51	1.02	−1.14	−1.15	30.69
7	hsa-miR-21 → MSH2	1.19	1.25	−1.42	−1.34	−1.64	−2.36
8	hsa-miR-106 → p21	2.25	1.09	1.14	1.06	−1.18	−1.84
9	hsa-miR-20	1.39	1.62	−1.23	1.38	−1.89	−1.34
10	hsa-miR-148a → GADD45	−1.94	−1.25	−1.41	1.19	−2.14	1.46
11	hsa-miR-370 → CLU/cyclin E2	10.55	7.51	1.85	−2.25	−6.82	−6.02
12	hsa-miR-326 → Tp73	4.14	8.16	−2.21	−1.37	−1.22	1.03
13	hsa-miR-128b	−1.95	−2.02	2.46	2.26	1.24	−1.56
14	hsa-miR-17-3p	−1.03	1.5	1.47	2.46	−1.63	−1.02

activity of oxaliplatin in a p53-dependent and p53-independent manner.

In the present study, we also found that HCT116 p53 null cells did not show an induction of p21waf1$^{/cip1}$ expression as measured in p53 wild type cells, suggesting that the lack of a functional p53 protein could lead to reduced p21 protein levels in response to oxaliplatin and satraplatin exposure. To clarify the role of p21$^{waf1/cip1}$ activation by mean of both drug treatments on elevated cytotoxicity, HCT116 p21$^{waf1/cip1}$ null cells were also tested. Satraplatin again exhibited a higher anti-proliferation effect on oxaliplatin compared to oxaliplatin. Indeed, the IC$_{50}$ value of satraplatin was 6 µM versus 37.5 µM for oxaliplatin (data not shown). This further suggests that the cells after satraplatin treatment endure apoptosis via a p21$^{waf1/cip1}$-independent pathway.

To better understand the apoptosis cascade, we evaluated cell death associated protein expression. It well known that p53 is mutated in more than 50% in colorectal tumours and has been shown to have a role in modulating tumour sensitivity to a wide number of chemotherapeutic agents [7]. Here, we show that satraplatin/oxaliplatin-induced apoptosis was associated with an up-regulation of p53 protein levels, detected at 48 h of treatment. Using HCT116 p53 null cells, we have shown that the targeted inactivation of p53 resulted in a threefold increase in the IC$_{50}$ in oxaliplatin- but not in satraplatin-treated cells. Based on the p53 null model, we demonstrated that loss of p53 may acquire resistance towards oxaliplatin but not towards satraplatin treatment. It was already published that cell types having a mutant or inactive p53 and/or Bax gene(s) show increased resistance to oxaliplatin treatment [7, 8].

Fig. 6 Effect of both drugs on cell death-related protein and microRNA expression of miR-34a. Equal protein amounts from unexposed cells have used as loading control and blot for actin served as normalization gene. **a** Basal protein levels of p53 downstream genes on cell death-related molecules of Bax, Bcl2, Bid and Fas on a representative colorectal cancer cells at 48-h treatment with 10 μM of oxaliplatin and satraplatin. **b** Pro and active caspase 8 after the treatment of cells with both drugs. **c** Fold change miRNA expression of hsa-miR-34a, which is inhibiting the transcription of Bcl2 and **d** semi-quantitative analysis of fold change to untreated control of Bcl2 protein expression following satraplatin and oxaliplatin treatments at 48 h
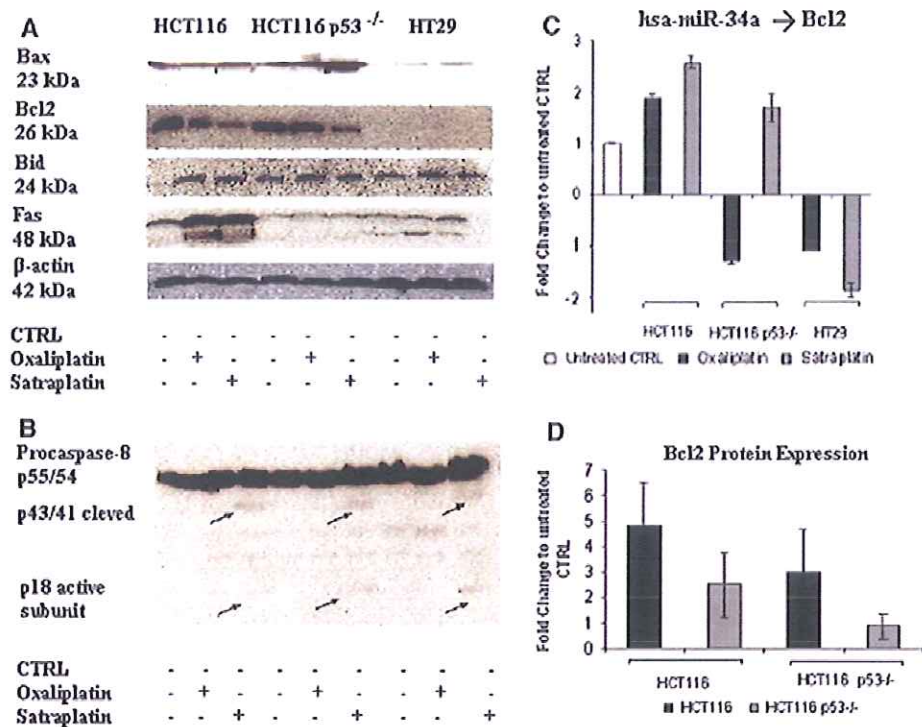
Furthermore, modulations of genes involved in the apoptosis response, such as Bax and Fas, are part of each platinum drug mode of action signature, indicating a common cell death mechanism [36]. We have demonstrated a down-regulation of Bcl2 and an up-regulation of Bax and Bid after exposure of both drugs in a subset of cell lines. These results demonstrate an important functional intrinsic pathway in the apoptotic cascade of events initiated by both drugs and are in agreement with previous publications [4]. We also observed that satraplatin induced an apoptotic response through activation of the extrinsic pathway by promoting Fas expression which in turn leads to the formation of the death-inducing signalling complex (DISC) and the auto-catalytic activation of pro-caspase 8. This phenomenon was further enforced by the involvement of the extrinsic pathway by oxaliplatin-induced apoptosis in colon cancer cells [38,39].

In addition to the basic molecular and biochemical analysis, we also examined the expression of certain miRNA on the response of cells to the platinum agent. MicroRNAs are small non-coding RNA molecules, which are able to control protein expression. It has been suggested that modification of miRNA gene expression could be another important factor in the responses to drug treatment [40]. As documented before, hsa-miR-34a was shown to induce apoptosis, cell cycle arrest, and senescence by p53-mediated activation [41]. Thus, we have detected high expression of miR-34a with satraplatin treatment than oxaliplatin in which miR-34a targeting Bcl2 protein

expression. In fact, we observed a lower expression of Bcl2 with satraplatin than oxaliplatin. In addition, we also detected a down-regulation of miR-214, which in turn targets Bax protein expression. This finding further suggests the role of miRNAs in chemotherapy responses based on p53-dependent and p53-independent routes.

In summary, this study highlights the molecular mechanisms underlying the cytotoxic effects of satraplatin for the first time in colorectal cancer cells in an attempt to identify different means of predicting response to this oral platinum agent. Our data suggest that the effect of satraplatin on proliferating colorectal cancer cells induces a G2/M cell cycle arrest and a molecular cascade of events consistent with an intrinsic–extrinsic mechanism of apoptosis. Moreover, the cytotoxic effects of satraplatin were shown to be both p53-dependent and p53-independent using an isogenic in vitro system. Further analysis is necessary to determine whether this orally available platinum agent has an effect in combination with other chemotherapy agents compared with oxaliplatin-based combinations. This could be a better solution for malignant cells that acquired resistance or de nova resistance against the currently available chemotherapy regimens.

References

1. Goldberg RM, Sargent DJ, Morton RF, Fuchs CS, Ramanathan RK et al (2004) A randomized controlled trial of fluorouracil plus leucovorin, irinotecan, and oxaliplatin combinations in patients with previously untreated metastatic colorectal cancer. J Clin Oncol 22:23–30

2. Hector S, Bolanowska-Higdon W, Zdanowicz J, Hitt S, Pendyala L (2001) In vitro studies on the mechanisms of oxaliplatin resistance. Cancer Chemother Pharmacol 48:398–406

3. Desoize B, Madoulet C (2002) Particular aspects of platinum compounds used at present in cancer treatment. Crit Rev Oncol Hematol 42:317–325

4. Gourdier I, Del Rio M, Crabbe L, Candeil L, Copois V, Ychou M, Auffray C, Martineau P, Mechti N, Pommier Y, Paul B (2002) Drug specific resistance to oxaliplatin is associated with apoptosis defect in a cellular model of colon carcinoma. FEBS Lett 529:232–236

5. Chen CC, Chen LT, Tsou TC, Pan WY, Kuo CC et al (2007) Combined modalities of resistance in an oxaliplatin-resistant human gastric cancer cell line with enhanced sensitivity to 5-fluorouracil. Br J Cancer 97:334–344

6. Lane DP (1992) p53, guardian of the genome. Nature 358:15–16

7. Arango D, Wilson AJ, Shi Q et al (2004) Molecular mechanism of action and prediction of response to oxaliplatin in colorectal cancer. Br J Cancer 91:1931–1946

8. Manic S, Gatti L, Carenini N, Fumagalli G, Zunino F, Perego P (2003) Mechanisms controlling sensitivity to platinum complexes: role of p53 and DNA mismatch repair. Curr Cancer Drug Targets 3:21–29

9. Mitsiades N, Yu WH, Poulaki V, Tsokos M, Stamenkovic I (2001) Matrix metalloproteinase-7-mediated cleavage of Fas ligand protects tumor cells from chemotherapeutic drug cytotoxicity. Cancer Res 61:577–581

10. Micheau O, Solary E, Hammann A, Martin F, Dimanche-Boitrel MT (1997) Sensitization of cancer cells treated with cytotoxic drugs to fas-mediated cytotoxicity. J Natl Cancer Inst 89:783–789

11. Peter ME, Legembre P, Barnhart BC (2008) Does CD95 have tumor promoting activities? Biochim Biophys Acta 1755:25–36

12. McKeage MJ (2005) New-generation platinum drugs in the treatment of cisplatin resistant cancers. Expert Opin Investig Drugs 14(8):1033–1046

13. Kelland LR, Abel G, McKeage MJ et al (1993) Preclinical antitumor evaluation of bis-acetato-ammine-dichloro-cyclohexylamine platinum (IV): an orally active platinum drug. Cancer Res 53:2581–2586

14. Sharp SY, Rogers PM, Kelland LR (1995) Transport of cisplatin and bis-acetato-ammine-dichlorocyclohexylamine platinum (IV) (JM-216) in human ovarian carcinoma cell lines: identification of a plasma membrane protein associated with cisplatin resistance. Clin Cancer Res 1(9):981–989

15. Moore MR, Troner MB, DeSimone P et al (1986) Phase II evaluation of weekly cisplatin in metastatic hormone-resistant prostate cancer: a southeastern cancer study group trial. Cancer Treat Res 70:541–542

16. McKeage MJ, Raynaud F, Ward J et al (1997) Phase I and pharmacokinetic study of an oral platinum complex given daily for 5 days in patients with cancer. J Clin Oncol 15:2691–2700

17. Fokkema E, Groen HJM, Bauer J et al (1999) Phase II study of oral platinum drug JM216 as first-line treatment in patients with small-cell lung cancer. J Clin Oncol 17:3822–3827

18. Fink D, Nebel S, Aebi S et al (1996) The role of DNA mismatch repair in platinum drug resistance. Cancer Res 56:4881–4886

19. Fokkema E, Groen HJM, Helder MN et al (2002) JM216, JM118, and cisplatin induced cytotoxicity in relation to platinum-DNA adduct formation, glutathione levels and p53 status in human cell lines with different sensitivities to cisplatin. Biochem Pharmacol 63:1989–1996

20. Sternberg CN, Whelan P, Hetherington P et al (2005) Phase III trial of satraplatin, an oral platinum plus prednisone versus prednisone alone in patients with hormone-resistant prostate cancer. Oncology 68:2–9

21. Vaisman A, Lim SE, Patrick SM et al (1999) Effect of DNA polymerases and high mobility group protein 1 on the carrier ligand specificity for translesion synthesis past platinum-DNA adducts. Biochemistry 38:11026–11039

22. Masters JRW, Twentyman P, Arlett C et al (2000) UKCCCR guidelines for the use of cell lines in cancer research. British J of Cancer 82(9):1495–1509

23. Matteucci C, Grelli S, De Smaele E, Fontana C, Mastino A (1999) Identification of nuclei from apoptotic, necrotic, and viable lymphoid cells by using multiparameter flow cytometry. Cytometry 35:145–153

24. Bustin SA, Benes V, Garson JA, Hellemans J, Huggett J, Kubista M et al (2009) The MIQE guidelines: minimum information for publication of quantitative real-time PCR experiments. Clin Chem 55(4):611–622

25. Blijham GH (1991) Chemotherapy of colorectal cancer. Anticancer Drugs 2:233–245

26. De Gramont A, Figer A, Seymour M et al (2000) Leucovorin and fluorouracil with or without oxaliplatin as first-line treatment in advanced colorectal cancer. J Clin Oncol 18:2938–2947

27. Kelland LR, Murrer BA, Abel G, Giandomenico CM, Mistry P, Harrap KR (1992) Ammine/amine platinum (IV) dicarboxylates: a novel class of platinum complexes exhibiting selective cytotoxicity to intrinsic cisplatin resistant human ovarian carcinoma cell lines. Cancer Res 52:822–828

28. Wosikowski K, Lamphere L, Unteregger G, Jung V, Kaplan F, Xu JP, Rattel B, Caligiuri M (2007) Preclinical antitumor activity of the oral platinum analog satraplatin. Cancer Chemother Pharmacol 60(4):589–600

29. Ormerod M, O'Neill C, Robertson D, Kelland LR, Harrap KR (1996) Cis-diamminedichloroplatinum(II)-induced cell death through apoptosis in sensitive and resistant human ovarian carcinoma cell lines. Cancer Chemother Pharmacol 37:463–471

30. Vaisman A, Varchenko M, Said I, Chaney SG (1997) Cell cycle changes associated with the formation of Pt-DNA adducts in human ovarian carcinoma cells with different cisplatin sensitivity. Cytometry 27:54–64

31. Zaffaroni N, Silvestrini R, Orlandi L, Bearzatto A, Gornati D, Villa R (1998) The induction of apoptosis by taxol and cisplatin and effect on cell cycle-related proteins in cisplatin, sensitive and resistant human ovarian cancer cells. Br J Cancer 77:1378–1385

32. O'Neill CF, Ormerod MG, Robertson D, Titley JC, Cumber-Walsweer Y, Kelland LR (1996) Apoptotic and non apoptotic cell death induced by cis and trans analogues of a novel ammine (cyclohexylamine) dihydroxodichloroplatinum (IV) complex. Br J Cancer 74:1037–1045

33. Sorenson CM, Eastman A (1998) Influence of cis-diamminedichloroplatinum (II) on DNA synthesis and cell cycle progression

in excision repair proficient and deficient Chinese hamster ovary cells. Cancer Res 48:6703–6707

34. Di Paola R (2002) To arrest or not to G2-M cell cycle arrest. Clin Can Res 8:3311–3314
35. Dan S, Yamori T (2001) Repression of cyclin B1 expression after treatment with Adriamycin, but not cisplatin in human lung cancer A549 cells. Biochem Biophys Res Commun 280:861–867
36. Voland C, Bord A, Peleraux A, Penarier G, Carriere D, Galiegue S, Cvitkovic E, Jbilo O, Casellas P (2006) Repression of cell cycle-related proteins by oxaliplatin but not cisplatin in human colon cancer cells. Mol Cancer Ther 5:2149–2157
37. Hata T, Yamamoto H, Ngan CY et al (2005) Role of p21$^{waf1/cip1}$ in effects of oxaliplatin in colorectal cancer cells. Mol Cancer Ther 4:1585–1594

38. Hayward RL, Macpherson JS, Cummings J, Monia BP, Smyth JF, Jodrell DI (2004) Enhanced oxaliplatin-induced apoptosis following antisense Bclxl down-regulation is p53 and Bax dependent: genetic evidence for specificity of the antisense effect. Mol Cancer Ther 3:169–178
39. Marchetti P, Galla DA, Russo FP, Ricevuto E, Flati V, Porzio G, Ficorella C, Cifone MG (2004) Apoptosis induced by oxaliplatin in human colon cancer HCT15 cell line. Anticancer Res 24:219–226
40. Rossi L, Bonmassar E, Faraoni I (2007) Modification of miR gene expression pattern in human colon cancer cells following exposure to 5-fluorouracil in vitro. Pharmacol Res 56(3):248–253
41. Hermeking H (2007) p53 enters the microRNA world. Cancer Cell 12(5):414–418